MNRAS **000**, 000–000 (0000) Preprint 17 March 2024 Compiled using MNRAS LATEX style file v3.0

Subpulse Drifting and Periodic Nulling in single pulse emission of PSR B2000+40

Rahul Basu[1], Wojciech Lewandowski[2], Jarosław Kijak[2]
[1] *Inter-University Centre for Astronomy and Astrophysics, Pune, 411007, India; rahulbasu.astro@gmail.com*
[2] *Janusz Gil Institute of Astronomy, University of Zielona Góra, ul. Szafrana 2, 65-516 Zielona Góra, Poland*

arXiv:2008.03329v1 [astro-ph.HE] 7 Aug 2020

17 March 2024

ABSTRACT

We have carried out a detailed study of single pulse emission from the pulsar B2000+40 (J2002+4050), observed at 1.6 GHz frequencies using the Effelsberg radio telescope. The pulsar has three components which are not well separated, with the central component resembling core emission. We have investigated modulations in single pulse behaviour using the fluctuation spectral analysis which showed presence of two prominent periodicities, around $2.5P$ and $40P$, respectively. The shorter periodicity was associated with the phenomenon of subpulse drifting and was seen to be absent in central core component. Drifting showed large phase variations in conal components. Additionally, the periodic modulations had significant evolution with time, varying between very sharp and highly diffuse features. In addition to drifting the pulsar also had presence of nulling in the single pulse sequence. The longer periodic feature in the fluctuation spectra was associated with nulling behaviour. The pulsar joins a select group which shows the presence of phase modulated drifting as well as periodic nulling in the presence of core emission. This provides further evidence for the two phenomena to be distinct from each other with different physical origin.

Key words: pulsars: individual: PSR B2000+40 (J2002+4050)

1 INTRODUCTION

The single pulse emission in normal period pulsars ($P > 0.1$ seconds) are characterised by the presence of different phenomena like subpulse drifting, nulling and mode changing (Drake & Craft 1968; Backer 1970, 1973). The pulsed radio emission is usually composed of one or more components called subpulses. In certain cases subpulses show systematic periodic variations within the pulse window and the phenomenon is known as subpulse drifting. Nulling and mode changing on the other hand is seen as large scale variations in the radio emission (Wang *et al.* 2007). During mode changing the pulsar emission switches between more than one stable state with different profile shapes. While nulling corresponds to the condition where the stable emission switches off and goes below detection limit for varying durations lasting from few periods, to hours and even months at a time in the case of intermittent behaviour (Kramer *et al.* 2006). An association between subpulse drifting and nulling behaviour was proposed with the discovery of periodic nulling (Herfindal & Rankin 2007, 2009). In certain pulsars it was observed that nulls, usually of short durations, were periodic in nature and co-existed with subpulse drifting whose periodicities were much shorter than nulling periodicity. This behaviour was explained using the carousel model where subpulse motion was associated with a rotating sub-beam system (Gil & Sendyk 2000; Deshpande & Rankin 2001). Periodic nulls were interpreted as empty line of sight (LOS) traverse between the sub-beam system and were termed as pseudo-nulls, distinguishing them from the general nulling phenomenon.

A systematic study of periodic behaviour in the single pulse sequences of pulsar population have been carried out in the recent past by Basu *et al.* (2016, 2017, 2019a, 2020a). A detailed classification of drifting behaviour revealed a close association with the profile type. The average radio emission beam is expected to consist of a central core component surrounded by concentric rings of conal emission. The average profile shape is believed to be closely associated with the LOS geometry across the emission beam (Rankin 1993). In case of tangential LOS traverses across the edge of the beam, the conal single (S_d) profile is observed. As the LOS cuts more interior regions of the beam, profile shapes become more complicated ranging from conal double (D), conal triple ($_c$T) and conal quadruple ($_c$Q). For central LOS traverses the core dominated profiles, core single (S_t), triple (T) and multiple (M) are seen. Subpulse drifting is seen to vary greatly across the different profile classes. The systematic coherent drifting with prominent drift bands and large phase variations are usually associated with peripheral LOS traverse of the emission beam in S_d and D profile classes. Drift behaviour becomes complicated for more interior LOS traverses, associated with $_c$T and $_c$Q profiles, where 180° phase jumps and phase reversals are seen across adjacent profile components. In the case of central LOS traverse, firstly, no drifting is seen in central core component, and secondly, in conal components prominent

© 0000 The Authors

drifting behaviour is observed which usually have low phase variations (Basu *et al.* 2019a).

These studies also reveal distinctions between subpulse drifting and other periodic phenomena like periodic amplitude modulation and periodic nulling seen in the single pulse sequence. In contrast to subpulse drifting periodic amplitude modulations and periodic nulling are not restricted to the subpulse behaviour, but are seen across the entire profile. Subpulse drifting is seen in pulsars with spin-down energy loss ($\dot{E}$) less than 2×10^{32} erg s^{-1}, and their periodicities are weakly anti-correlated with $\dot{E}$ (Basu *et al.* 2016, 2019a), i.e. pulsars with lower $\dot{E}$ tend to have higher drifting periodicities and vice versa. On the other hand periodic nulling and periodic amplitude modulation are seen over a wide $\dot{E}$ range, much higher than the drifting boundary, and do not show any dependence on $\dot{E}$ (Basu *et al.* 2017, 2020a). This has prompted the assertion that they are a newly emergent phenomenon in pulsars distinct from subpulse drifting (Basu *et al.* 2017, 2020a). Additionally, a clear distinction is seen in relation to the behaviour of core emission. As noted earlier subpulse drifting is not seen in the core, while the periodic modulations are seen across the entire profile including the core. There are only three pulsars with prominent core emission which show the presence of both subpulse drifting as well as periodic modulations in their pulse sequence, PSR J1239+2453 (Smith *et al.* 2013; Maan & Deshpande 2014; Basu *et al.* 2020a), PSR J1740+1311 (Force & Rankin 2010) and PSR J2006−0807 (Basu *et al.* 2019b). All the three pulsars have M profile type, with PSR J1239+2453 and J2006−0807 showing periodic nulling, while PSR J1740+1311 exhibit periodic amplitude modulation.

The above discussion signifies the importance of studying periodic behaviour in pulse sequences particularly in presence of a central core component. The primary focus of this work is to carry out detailed analysis of single pulse behaviour of the pulsar B2000+40 (J2002+4050) which has three components, with the central component resembling core emission. The presence of subpulse drifting at 21 cm observing wavelength was reported for this source by Weltevrede *et al.* (2006). However, no drifting behaviour could be seen at 92 cm observations of Weltevrede *et al.* (2007) as well as the 333 MHz studies of Basu *et al.* (2019a). The low radio frequency observations had lower detection sensitivities of single pulses and were likely affected by scattering effects in the intervening medium. There were indications of low frequency features corresponding to periodic intensity modulations in the 333 MHz observations, but they could not be confirmed. This prompted us to carry out a detailed study of this source at a higher frequency. We have carried out a thorough analysis of the radio emission from this pulsar. In section 2 we present the observational setup and analysis scheme used to generate the single pulse sequence. Section 3 details the behaviour of the average profile while sections 4 and 5 presents the single pulse analysis leading to the characterisation of subpulse drifting and nulling, respectively. A discussion of the implications of the results of this study is presented in section 6 followed by a short summary and conclusions in section 7.

2 OBSERVATION AND ANALYSIS

The data presented here is a part of an observing project that involved single pulse observations of eight strong northern hemisphere pulsars. The observations were performed with the 100-meter Effelsberg radio telescope between March 9 and March 11, 2018. Data was acquired using the L-band receiver with the central frequency of 1635 MHz with a bandwidth of 250 MHz. Each pulsar

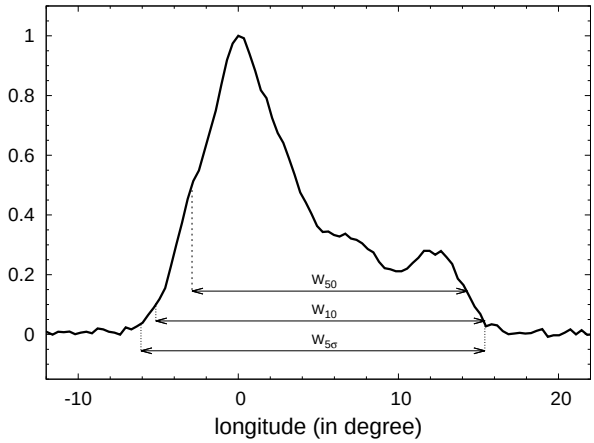


Figure 1. The figure shows average profile of PSR J2002+4050 at 1.6 GHz. The profile shows presence of three components, with the leading conal component being the dominant one and not clearly separated from the central core emission. The boundaries corresponding to the profile widths $W_{5\sigma}$, W_{10} and W_{50} are also shown n the figure.

Table 1. Measuring Profile widths of PSR J2002+4050

$W_{5\sigma}$ (°)	W_{10} (°)	W_{50} (°)	W_{SEP}^{cone} (°)
21.5±0.4	20.6±0.4	17.2±0.4	12.1±0.4

was observed for a minimum of ten thousand individual pulses. The Effelsberg pulsar recording machine PSRIX (Lazarus *et al.* 2016) was used to record coherently dedispersed data and then to translate it into 128 frequency channels and between 1024 and 4096 phase bins depending on a pulsar period (2048 bins in the case of PSR J2002+4050), in a single-polarization mode (i.e. total intensity only). Data were saved in the ARCHIVE format for each pulse separately and then merged to create a single file.

The next steps of the analysis, including the interference (RFI) cleaning process was performed with the help of the PSRCHIVE package (Hotan *et al.* 2004). The narrow band interference was removed using a median filter as implemented by the "zap" routine in PSRCHIVE (van Straten *et al.* 2012). Due to heavy interference we were forced to remove more than a half of the spectral channels, reducing the effective bandwidth to about 100 MHz. Initial 30 percent and around 10 percent of the bandwidth at the end was removed due to RFI. Additional, 10-20 percent of spectral channels distributed within the remaining band were also affected by narrow band RFI. The effective central frequency was around 1660 MHz. After the interference removal the data was dedispersed to create the total intensity time series and translated into the ASCII format for further processing.

3 AVERAGE PROFILE BEHAVIOUR

We have estimated the average profile of the pulsar at 1.66 GHz observing frequency which is shown in figure 1. The profile shows presence of three components, with the leading component being the most prominent having peak intensity more than three times the other two components. The different components in the pro-

file are not clearly separated at the observing frequency with the central component being merged with the leading one. In Table 1 we have estimated the profile widths as well as separation between the peaks of the two conal components (W_{SEP}^{cone}). The peak location of the leading component was seen in the average profile. However, the peak location of the trailing component was not clearly identified and the centroid was used. Three separate estimates were carried out for the profile width as shown in figure 1. $W_{5\sigma}$ was the separation between the two longitudes at the leading and trailing edge of the profile that were five times the baseline noise rms level. Additionally, we also estimated W_{10} and W_{50}, which corresponded to separation between 10 percent peak intensity level of the leading and trailing components and the 50 percent peak intensity levels of the two components. We have not come across any clear classification of this pulsar profile in the literature. The observational setup did not allow us to estimate polarization behaviour. However, the polarization in the average profile has been reported in earlier works (Gould & Lyne 1998). The polarization position angle suggests large swing across the pulsar profile consistent with a central line of sight traverse (Radhakrishnan & Cooke 1969). There are also indications of orthogonal polarization modes which has important implications for understanding the emission mechanism (Mitra *et al.* 2009; Melikidze *et al.* 2014). The linear polarization shows depolarization effect towards the profile edges while the circular polarization show sign changing behaviour near the central component. The above features are consistent with core-cone T profile type. The drifting behaviour reported in section 4 provides additional support for this profile classification.

4 PERIODIC MODULATIONS OF SINGLE PULSES

We have used the fluctuation spectral analysis to estimate periodic modulations in the single pulse sequence. The details of the analysis is reported in Basu & Mitra (2018a), which is briefly summarized as follows. The longitude resolved fluctuation spectra (LRFS, Backer 1973) was estimated for 256 consecutive periods. The LRFS was estimated at regular intervals, from the beginning of observations and subsequently shifting the starting pulse by fifty periods. The average LRFS amplitude, across all longitudes along the pulse window, was represented as a function of the starting period to determine the time evolution of periodic modulations. The time evolution of LRFS is shown in figure 2, left panel, which shows the presence of two distinct peaks in the fluctuation spectra. In addition to the time evolution of the amplitude, averaged for all longitudes, we have also estimated the variation of periodic behaviour across the pulse window. This was determined for the high frequency feature associated with subpulse drifting. The distribution of peak fluctuation amplitude at each longitude is shown in figure 2, top window of right panel (red points), along with the average behaviour (black points). Additionally, we have also estimated the distribution of relative phase variations corresponding to the drifting peak, which is shown in the middle window of the plot. The relative phase variations were estimated for each LRFS, with the phases corresponding to the profile peak fixed at zero. The peak amplitudes and phases were represented for significant detections, where the drifting peak exceeded three times the rms level of the baseline. The single pulse sequence during our observations were affected by RFI which were likely to introduce artificial peaks in the fluctuation spectra. To mitigate such behaviour we identified a window of same width as the profile in the off-pulse region and estimated the LRFS corresponding to this window. The RFI being terrestrial in origin was present throughout the profile and not just in the pulse window. Subsequently, the LRFS in the off-pulse window was subtracted from the LRFS of pulse window which suppressed the peaks arising due to RFI. In none of these cases the RFI peaks were coincident with the modulation periodicities of the pulsar emission.

Table 2. Estimating periodic behaviour in PSR J2002+4050

	f_p	FWHM	S_M	P_M	$d\phi/d\psi$ COMP-1	$d\phi/d\psi$ COMP-3
	(cy/P)	(cy/P)	(P/cy)	(P)	($^\circ$/$^\circ$)	($^\circ$/$^\circ$)
Drift.	0.396±0.018	0.042	12.6	2.52±0.11	41.1±3.0	27.9±3.0
Per. Null	0.025±0.007	0.017	41.3	39.6±11.6	...	...

As shown in figure 2, left panel, there are two distinct periodic features in the single pulse sequence. The average periodic behaviour does not appear to be very sharp in both cases and show significant variations with time. This appears to be a general behaviour of subpulse drifting as well as other periodic modulations, as noted in a number of other pulsars (Basu *et al.* 2017; Basu & Mitra 2018a). These variations are highlighted in the LRFS estimated for the two specific intervals shown in figure 3. The left panel corresponds to the sequence between pulse number 4000 and 4256 from the start of the observations. The LRFS shows presence of a very sharp peak corresponding to subpulse drifting, but the low frequency feature is very weak in this sequence. The right panel shows the LRFS corresponding to the sequence between pulses 1000 and 1256. The drifting behaviour is seen as a diffuse structure in this duration while the low frequency behaviour becomes much more prominent. Table 2 reports estimates of peak features corresponding to the two phenomena from time average fluctuation spectra. The Table shows peak frequency (f_p), full width at half maximum (FWHM) of each feature, strength of each peaks (S_M) given by the maximum height from baseline level divided by FWHM, and corresponding periodicities (P_M). The error in estimating peak frequency is obtained using a Gaussian approximation, $\delta f_p = \mathrm{FWHM}/2\sqrt{2\ln 2}$ (Basu *et al.* 2016).

The low frequency feature around periodicity of 40 P corresponds to periodic nulling and is explored in detail in section 5. The high frequency feature with P_3 around 2.5 P arises due to subpulse drifting. As seen in figure 2, right panel, subpulse drifting is only seen in the conal components and is completely absent in the central core emission. In the first conal component drifting is seen primarily in the leading part and is greatly diminished near the trailing edge. The leading component is not clearly separated from the core emission and it is possible that the trailing part of the component is affected by the lack of drifting in the core, thereby curtailing the drifting behaviour. Subpulse drifting in conal components are also characterised by large phase variations. This is not usual for central LOS traverses of the emission beam which are mostly accompanied by low phase variations (Basu *et al.* 2019a). We have estimated rate of variations of drift phase (ϕ) with the pulse longitude (ψ), which is represented as $d\phi/d\psi$ in Table 2, by linear approximation of the phase variations in each conal component. The leading conal component shows larger drift phase variations compared to the trailing component. The drift rate can also be estimated using this measurement as $D_R = 360^\circ/(P_3 \times d\phi/d\psi)$. The average drift rate is 3.5±0.4 $^\circ/P$ for the leading conal component and 5.1±0.8 $^\circ/P$ for the trailing component.

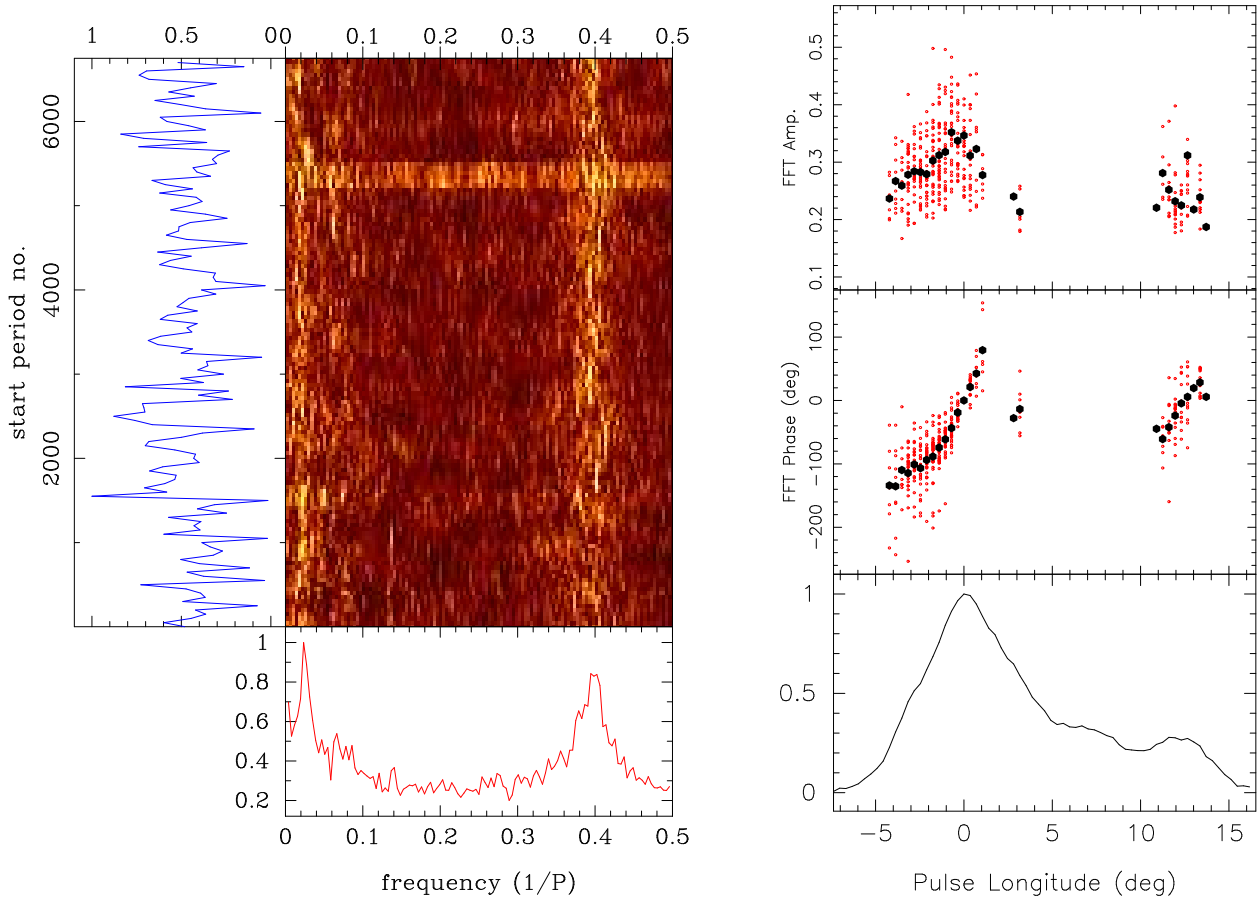


Figure 2. The figure shows fluctuation spectral analysis on single pulse sequence of PSR J2002+4050. The left panel shows time variation of the Longitude resolved fluctuation spectra (LRFS). The bottom window represents average LRFS across all times and shows presence of two clear peaks. The low frequency peak corresponds to periodic nulling while the high frequency peak arises due to subpulse drifting. The right panel shows variation of the drifting behaviour across the pulse profile. The top window shows the variation of the peak drifting amplitude while the middle window represents the average phase behaviour corresponding to drifting peak. Subpulse drifting is absent in the central core component. The conal components on the other hand show large phase variations.

5 NULLING

We have detected the presence of nulling in the single pulse sequence of this pulsar. In figure 4 a short interval of the pulse sequence, around 150 pulses, is shown which reflects the nulling behaviour. The figure shows that the pulsar goes to null state where the radio emission vanishes for short durations lasting between 5-10 P at a time. In order to characterise the nulling behaviour we have determined the pulse energy distribution which is shown in figure 5. The average energy in the pulse window was estimated for each single pulse along with baseline average in a suitably selected off-pulse window. The histograms of the energy distributions were estimated in each case after normalizing the x-axis with average on-pulse energy and the y-axis with total number of pulses. The pulse energy distribution shows presence of a bimodal structure with lower part corresponding to null pulses. The nulling fraction was determined by fitting Gaussian functions to off-pulse and null distributions and estimating the ratio between the two (Ritchings 1976). The pulsar was in the nulling state for 11.5±0.4 percent of time during the duration of our observations. One of the drawbacks of these estimates is the relatively low detection sensitivity of the single pulse emission. This is also highlighted in the pulse energy distribution where null and burst distributions are not well separated. As a result it was impossible to identify the null pulses statistically and carry out a more detailed analysis of the nulling behaviour, like estimating the null and burst length distribution, as well as searching for any low level emission during nulling.

One of the features of the fluctuation spectral analysis reported in the previous Section is the presence of low frequency feature around 0.025 cy/P. The presence of nulling gives rise to the possibility that the feature is indicative of periodic nulling behaviour in the pulsar. Although, low sensitivity of single pulse detection makes it impossible to identify the null and burst pulses statistically, figure 4 shows that it is still possible to identify null regions by visually inspecting the pulse sequence. We have employed this technique to largely identify the null and burst regions and carry out a periodicity analysis similar to Basu *et al.* (2017). This involved setting up a binary sequence where the null pulses were identified as '0' and the burst pulses as '1'. Subsequently, Fourier transforms of this series were carried out, similar to the fluctuation spectral analysis, using 256 points at a time, and continuously shifting the start period by 50 pulses. The time evolution of the nulling FFT is shown in figure 6, left panel, where the average spectra shows the presence of a low frequency peak at f_p = 0.027 cy/P. Firstly, the above analysis clearly demonstrates nulling to be periodic in nature, and secondly, the peak frequency in nulling FFT is coincident with the low frequency feature in fluctuation spectra indicating a

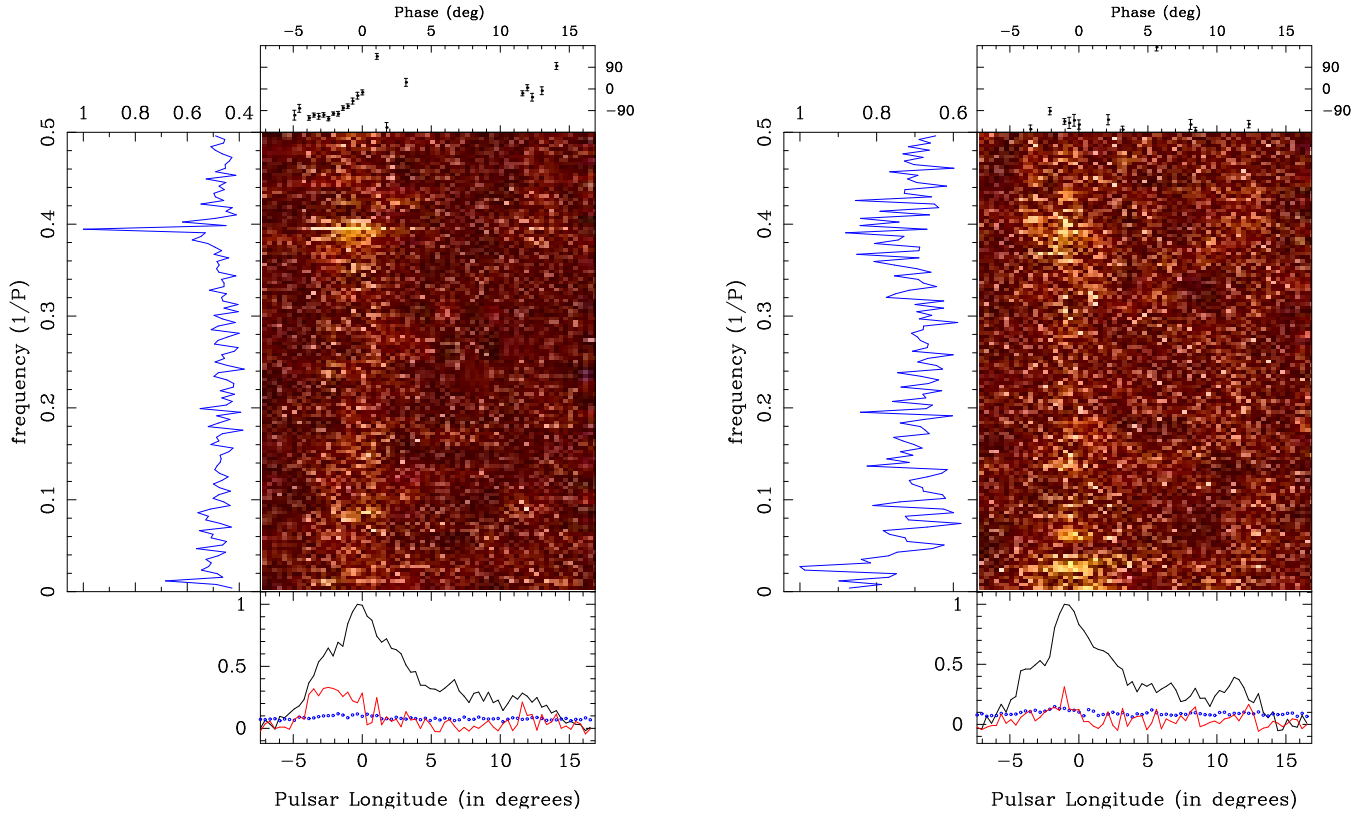


Figure 3. The figure shows variation of LRFS for the pulsar J2002+4050 during two intervals within the pulse sequence. The left panel corresponds to interval between pulse 4000 and 4256 and shows presence of a sharp feature corresponding to subpulse drifting. The right panel corresponds to interval between pulse 1000 and 1256 and shows presence of diffuse drifting. The low frequency modulations on the other hand are more prominent in this interval.

common origin for both. As a result we can conclusively ascertain that the longer periodic modulations detected in the single pulse sequence of this pulsar is indeed due to periodic nulling. To further demonstrate the validity of this claim we show the fluctuation spectra in a region of the pulse sequence, between pulse number 3100 and 3400, where relatively fewer nulls were visible. The low frequency feature is not seen in LRFS as expected. The periodic behaviour is also indicated in the pulse sequence in figure 4, where the interval between onset of nulls vary between 30 to 40 P which matches with the measured periodicity in the fluctuation spectra. However, it should also be noted that the nulling FFT shown in figure 6 is not an exact representation of the periodic behaviour since a number of null pulses, particularly single period nulls, were not likely to be identified due to the limitations of these observations, which may result in suppression of high frequency features in the nulling FFT.

6 DISCUSSION

The pulsar J2002+4050 joins a small, but increasing, group of sources which show the presence of both periodic nulling as well as subpulse drifting in their pulse sequences. A survey of such sources has been conducted recently by Basu *et al.* (2020a), where around 20 pulsars are reported to show the presence of both low frequency periodic modulation and subpulse drifting. Amongst them the more relevant cases are the ones where there is a central core emission. There are only three such pulsars, PSR J1239+2453, J1740+1311 and J2006−0807, all of which have a five component M type profile. In case of the pulsars J1239+2453 (Basu *et al.* 2020a) and J2006−0807 (Basu *et al.* 2019b) the low frequency feature corresponds to periodic nulling while in PSR J1740+1311 (Force & Rankin 2010) there are few nulls and the pulsar exhibit periodic amplitude modulation. PSR J2002+4050 is the first known example of a core-cone T profile where the conal components show the presence of subpulse drifting in addition to the presence of periodic nulls. In this context it is interesting to explore the periodic behaviour in PSR J2002+4050.

As noted earlier subpulse drifting in PSR J2002+4050 shows large phase variations which are not common in pulsars with central LOS traverses, where generally flat phase variations are seen (Basu *et al.* 2019a). However, there are examples of large phase variations associated with certain conal emission in some cases. The pulsar J1239+2453 (Maan & Deshpande 2014; Smith *et al.* 2013; Basu *et al.* 2019a) shows large phase variations in the second conal component while the first and fifth components show largely phase stationary behaviour. The drifting in the fourth component is weaker and the phase behaviour is not clearly seen. Similarly, in the case of PSR J2006−0807 the outer conal components show phase stationary behaviour with very little change, while the inner cones show large phase variations. However, the phase variations in the inner cones show the interesting phenomenon of bi-drifting where the drift directions, and consequently the phase slopes, are opposite in nature. The large phase variations seen associated with the drifting in PSR J2002+4050 seem to indicate that the conal components resemble the inner cones of the M type pro-

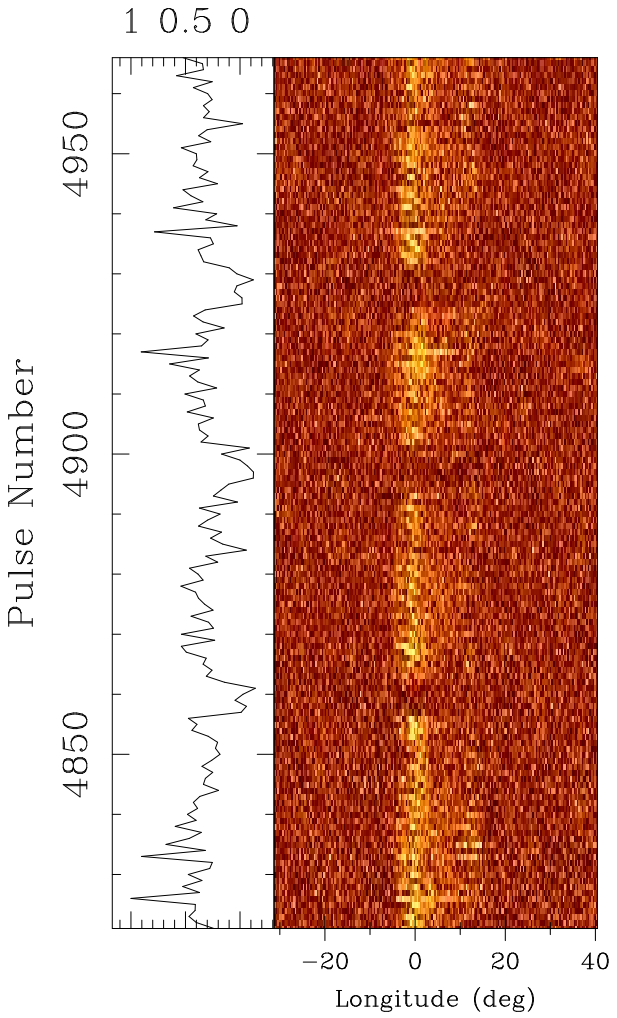


Figure 4. The figure shows a section of single pulse sequence of pulsar J2002+4050, between pulse number 4820 and 4970 from the start of the observing session. The pulsar shows presence of nulling at regular intervals. The figure shows presence of three prominent nulling regions around pulse 4860, 4900 and 4930. The left window shows average energy corresponding to each single pulse, where the peak energy is normalized to unity. The energy drops to baseline noise levels during nulling intervals.

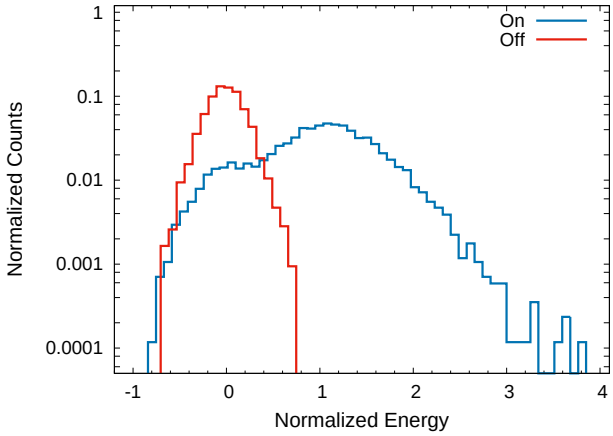


Figure 5. The figure shows the pulse energy distribution corresponding to on-pulse (blue) and off-pulse (red) window. The on-pulse distribution shows a bimodal structure, where the lower part of distribution is coincident with off-pulse histogram. This indicates the presence of nulling in the pulsar J2002+4050.

files. This is further highlighted by the fact that the components are not clearly separated. However, unlike PSR J2006−0807, the phase variations in the two components are not in the opposite directions, despite, the slope in the leading component being much steeper than the trailing component.

The coherent radio emission originates due to non-linear instabilities in non-stationary, relativistic, outflowing plasma clouds moving along the open magnetic field lines (Asseo & Melikidze 1998; Melikidze *et al.* 2000; Mitra *et al.* 2009; Lakoba *et al.* 2018; Rahaman *et al.* 2020). The non-stationary plasma clouds are generated due to sparking discharges in an inner acceleration region (IAR) above the stellar surface, and requires presence of non-dipolar magnetic fields (Ruderman & Sutherland 1975; Gil & Sendyk 2000; Mitra *et al.* 2020). The sparks undergo variable $\mathbf{E} \times \mathbf{B}$ drift due to presence of large electric and magnetic fields in IAR which is imprinted in the outflowing plasma and seen as subpulse drifting in the radio emission. The phase variations seen associated with subpulse drifting in central LOS pulsars are particularly challenging to understand from the perspective of Ruderman & Sutherland (1975) model of sparks rotating around the dipolar magnetic axis. Subsequent studies have introduced the concept of elliptical emission beams with axes tilted with respect to the fiducial plane in order to explain these phase variations (Wright & Weltevrede 2017). The physical origin of these tilted structures were explained by Szary & van Leeuwen (2017); Szary *et al.* (2020) by introducing the effect of non-dipolar fields in the polar cap which shifts it from the canonical dipolar location. It was suggested that the plasma in the IAR rortate around a point of maximum potential at the polar cap. However, Basu *et al.* (2020b) showed that in the absence of any external electric field, the variable $\mathbf{E} \times \mathbf{B}$ drift in the IAR causes the sparks to lag behind the co-rotation motion of the pulsar, which is around the rotation axis. The non-dipolar polar cap is shifted from purely dipolar case, but in the emission region, around heights of few hundred kilometers from the surface, the magnetic field is purely dipolar in nature (Kijak & Gil 1997, 2003; Mitra & Rankin 2002; Krzeszowski *et al.* 2009; Mitra 2017). As the non-dipolar magnetic field line in the polar cap surface connects with the dipolar fields in the emission region, the field lines get twisted and the LOS traverses the sparks at different angles depending on the nature of the surface field. In case of pulsars like J2002+4050 with a central core component and large drifting in the cone, it was found that the non-dipolar polar cap located on the sides of the neutron star relative to the dipolar case, i.e. roughly 90° away, is a likely configuration for the drifting behaviour. However, more detailed modelling is required to explain the drifting phase behaviour in J2002+4050, particularly the different drift rates in the two conal components, etc. Other examples of similar behaviour needs to be uncovered in the pulsar population to find additional constraints on the physical models explaining the subpulse drifting in central LOS traverse systems.

A number of studies in the recent past (Basu *et al.* 2016; Mitra & Rankin 2017; Basu *et al.* 2017; Basu & Mitra 2018b; Basu *et al.* 2019a,b; Basu & Mitra 2019c; Basu *et al.* 2020a; Yan *et al.* 2019, 2020) have highlighted the physical differences between subpulse drifting and low frequency modulations corresponding to periodic nulling and periodic amplitude modulation.

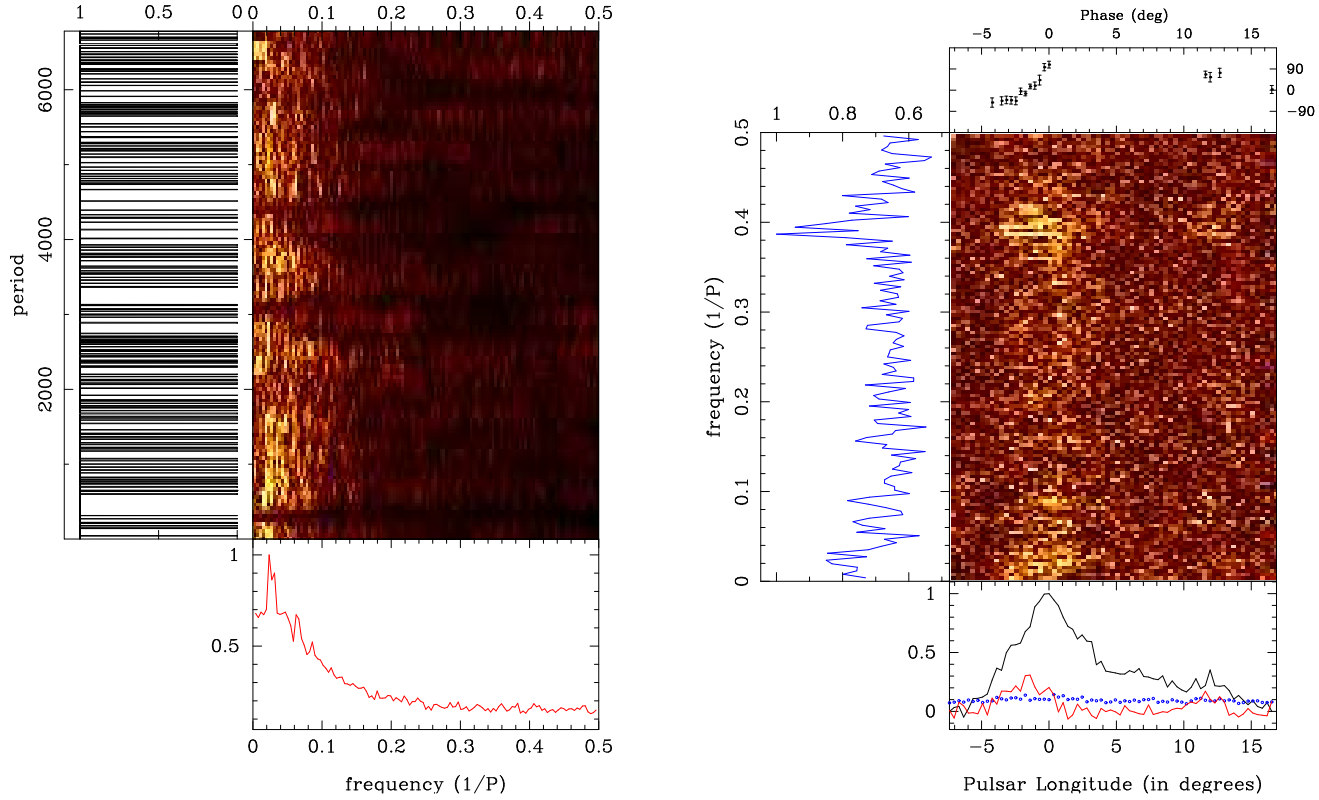


Figure 6. The left panel of the figure shows time evolution of FFT corresponding to the null/burst time series. The nulls and burst pulses were identified as 0 and 1, as shown in the left window, and a continuous FFT of the sequence was measured. The average FFT over the entire sequence is estimated in the bottom window which shows the presence of a low frequency feature around 40 P. The peak frequency is coincident with the low frequency feature in the average fluctuation spectra. The right panel in the figure corresponds to the fluctuation spectra between pulse 3100 and 3400 where very little clear nulls are seen (see left panel). The absence of clear low frequency feature in the LRFS further suggests the longer periodicity modulation to be due to periodic nulling.

The subpulse drifting is only associated with conal components while the entire pulsar emission is simultaneously affected by periodic modulations. The differences in the behaviour is clearly reflected in the single pulse emission of PSR J2002+4050 where the subpulse drifting is absent in the central core component. The core component is merged with the leading conal component, whose trailing edge also seems to be affected by the core where drifting effect is significantly reduced. Nulling is not clearly distinguishable from low S/N single pulses, except during longer (∼5 to 10 P) nulling intervals where the radio emission from all three components appears to vanish. It is possible that the pulsar goes to a low level emission state similar to PSR J1048−5832 (Yan *et al.* 2020), rather than a complete null, which will require more sensitive future observations to uncover. The two periodic phenomena also differ in their dependence on the spin-down energy loss ($\dot{E}$). The subpulse drifting is only seen in pulsars with $\dot{E} < 2{\times}10^{32}$ erg and the drifting periodicity is weakly anti-correlated with $\dot{E}$, implying that for higher values of $\dot{E}$ the P_3 is generally lower. The best fit values to the $P_3 - \dot{E}$ correlation was estimated by Basu *et al.* (2016) as $P_3 = (\dot{E}/2.3{\times}10^{32})^{-0.6}$. The pulsar J2002+4050 has $\dot{E}$ of $9.26{\times}10^{31}$ erg s^{-1} (Hobbs *et al.* 2004), which is near the upper boundary but does not exceed it. The estimated P_3 of $2.5P$ is relatively low and the corresponding aliased value P_3^a is $1.66P$. The expected P_3 from the above correlation is $1.72P$ which suggests the aliased periodicity is a better fit to the correlation. However, there is large scatter in the $P_3 - \dot{E}$ distribution which makes such associations tentative. On the other hand the low frequency periodic modulations do not show any clear dependence on $\dot{E}$ and have periodicities which appear in a relatively wide band with P_M between 10-200P (Basu *et al.* 2020a). The periodic nulling in PSR J2002+4050 has P_M of around $40P$ which is also consistent with expected behaviour. The periodic modulations observed in the single pulse sequence of this pulsar provides further evidence that the periodic nulling originate due to different physical mechanism compared to subpulse drifting.

7 SUMMARY AND CONCLUSION

We have carried out a detailed analysis of the single pulse emission from the core-cone Triple pulsar J2002+4050, observed around 1.6 GHz frequencies using the Effelsberg radio telescope. The single pulse sequence showed the presence of periodic modulations at two different timescales, $2.5P$ corresponding to the phenomenon of subpulse drifting and $40P$ arising due to periodic nulling. Subpulse drifting was seen only in the two conal components but was absent in the central core emission. Unlike the majority of pulsars with central line of sight traverse of the emission beam, the drifting in this case showed large phase variations across both conal components. The periodic modulation features corresponding to both these phenomena showed variations with time where they had sharp features at certain instances which became diffuse at other times. We have also detected the presence of nulling for the first time in this pulsar. The pulsar was in the null state for 11.5 percent of the

observing durations. We were not able to statistically identify the null pulses due to the low sensitivity of detection of single pulses, however, there were regular intervals of nulling lasting between 5-10 periods which could be identified by visual inspection. These nulling durations were demonstrated to exhibit periodic behaviour which was coincident with the $40P$ modulations seen in the pulse sequence. The periodic nulling and subpulse drifting are expected to arise due to different physical mechanisms. Our analysis for the pulsar J2002+4050 provides further evidence to demonstrate the distinction between the two phenomena.

ACKNOWLEDGMENTS

We thank Dr. Ramesh Karuppusamy for his assistance with technical issues during the observations. We also thank Dr. Karolina Rożko and Sławomir Białkowski for their assistance with the observations. R.B. thanks Dr. Dipanjan Mitra and Prof. George I. Melikidze for useful discussions. This work is based on observations with the 100-m telescope of the MPIfR (Max-Planck-Institut für Radioastronomie) at Effelsberg. This work has received funding from the European Union's Horizon 2020 research and innovation program under grant agreement No 730562 [RadioNet].

DATA AVAILABILITY

The time series single pulse data for PSR J2002+4050 in ascii format underlying this article will be shared on reasonable request to the corresponding author.

REFERENCES

Asseo, E.; Melikidze, G.I. 1998, MNRAS, 301, 59
Backer, D.C. 1970, Nature, 228, 42
Backer, D.C. 1973, ApJ, 182, 245
Basu, R.; Mitra, D.; Melikidze, G.I.; Maciesiak, K.; Skrzypczak, A.; Szary, A. 2016, ApJ, 833, 29
Basu, R.; Mitra, D.; Melikidze, G.I. 2017, ApJ, 846, 109
Basu, R.; Mitra, D. 2018a, MNRAS, 475, 5098
Basu, R.; Mitra, D. 2018b, MNRAS, 476, 1345
Basu, R.; Mitra, D.; Melikidze, G.I.; Skrzypczak, A. 2019a, MNRAS, 482, 3757
Basu, R.; Paul, A.; Mitra, D. 2019b, MNRAS, 486, 5216
Basu, R.; Mitra, D. 2019c, MNRAS, 487, 4536
Basu, R.; Mitra, D.; Melikidze, G.I. 2020a, ApJ, 889, 133
Basu, R.; Mitra, D.; Melikidze, G.I. 2020b, MNRAS, in press.
Deshpande, A.A.; Rankin, J.M. 2001, ApJ, 322, 438
Drake, F.D.; Craft, H.D. 1968, Nature, 220, 231
Force, M.M.; Rankin, J.M. 2010, MNRAS, 406, 237
Gil, J.; Sendyk, M. 2000, ApJ, 541, 351
Gould, D.M.; Lyne, A.G. 1998, MNRAS, 301, 235
Herfindal, J.L.; Rankin, J.M. 2007, MNRAS, 380, 430
Herfindal, J.L.; Rankin, J.M. 2009, MNRAS, 393, 1391
Hobbs, G.; Lyne, A.G.; Kramer, M.; Martin, C.E.;Jordan, C. 2004, MNRAS, 353, 1311
Hotan, A.W., van Straten, W., Manchester, R.N. 2004, Publications of the Astronomical Society of Australia, 21, 302
Kijak, J.; Gil, J. 1997, MNRAS, 288, 631
Kijak, J.; Gil, J. 2003, A&A, 397, 969
Krzeszowski, K.; Mitra, D.; Gupta, Y.; Kijak, J.; Gil, J.; Acharyya, A. 2009, MNRAS, 393, 1617
Kramer M.; Lyne A.G.; O'Brien J.T.; Jordan C.A.; Lorimer D.R. 2006, Science, 312, 549
Lakoba, T.; Mitra, D.; Melikidze, G. 2018, MNRAS, 480, 4526
Lazarus, P., Karuppusamy, R., Graikou, E., Caballero, R.N. , Champion, D.J., Lee, J.K., Verbiest, J P.W., Kramer, M. 2016, MNRAS, 458, 868
Maan, Y.; Deshpande, A.A. 2014, ApJ, 792, 130
Melikidze, G.I.; Gil, J.A.; Pataraya, A.D. 2000, ApJ, 544, 1081
Melikidze, G.I.; Mitra, D; Gil, J.A. 2014, ApJ, 794, 105
Mitra, D., Rankin, J.M. 2002, ApJ, 577, 322
Mitra, D.; Gil, J.; Melikidze, G. 2009, ApJL, 696, L141
Mitra, D.; Rankin, J. 2017, ApJ, 468, 4601
Mitra, D. 2017, JApA, 38, 52
Mitra, D.; Basu, R.; Melikidze, G.I.; Arjunwadkar, M. 2020, MNRAS, 492, 2468
Radhakrishnan, V.; Cooke, D.J. 1969, ApL, 3, 225
Rahaman, Sk. M.; Mitra, D.; Melikidze, G.I. 2020, accpeted in MNRAS, eprint arXiv:2007.15395
Rankin, J.M. 1993, ApJ, 405, 285
Ritchings, R.T. 1976, MNRAS, 176, 249
Ruderman, M.A.; Sutherland, P.G. 1975, ApJ, 196, 51
Smith, E.; Rankin, J.M.; Mitra, D. 2013, MNRAS, 435, 1984
Szary, A.; van Leeuwen, J. 2017, ApJ, 845, 95
Szary, A.; van Leeuwen, J.; Weltevrede, P.; Maan, Y. 2020, ApJ, 896, 168
van Straten, W., Demorest, P., Oslowski, S. 2012, Astronomical Research and Technology, 2012, Vol.9 No.3, 237
Wang, N.; Manchester, R.N.; Johnston, S. 2007, MNRAS, 377, 1383
Weltevrede, P.; Edwards, R. T.; Stappers, B. W. 2006, A&A, 445, 243
Weltevrede, P.; Edwards, R. T.; Stappers, B. W. 2007b, A&A, 469, 607
Wright, G.; Weltevrede, P. 2017, MNRAS, 464, 2597
Yan, W.M.; Manchester, R.N.; Wang, N.; Yuan, J.P.; Wen, Z.G.; Lee, K.J. 2019, MNRAS, 485, 3241
Yan, W.M.; Manchester, R.N.; Wang, N.; Wen, Z.G.; Yuan, J.P.; Lee, K.J.; Chen, J.L. 2020, MNRAS, 491, 4634